A Novel Hydrogen Storage Power Plant Structure for High Renewable Energy Penetration

Nayeemuddin Ahmed[1] and Harald Weber[1]
[1]Electrical Energy Supply (EEV), University of Rostock, Germany
nayeemuddin.ahmed@uni-rostock.de

Abstract

Integration of increasing magnitudes of renewable energy is of paramount importance to find an alternative to diminishing non-renewable fossil fuels and reduce the emission of greenhouse gases to agreed levels. However, including higher proportions of such energy sources introduces new challenges for grid operators. Electrical power generation dependent on intermittent renewable resources can easily lead to situations with large differences between forecasted and actual values of power generation and consumption. This would signal the need for power curtailment or a sizeable dispatch of emergency power reserves. A feasible method of large-scale energy storage is required to bridge this gap between stochastic generation and consumption. The Hydrogen Storage Power Plant (HSPP) is one such solution.

In this paper, a novel structure of the HSPP consisting of storages and DC-AC converters (HSPP-AC) is proposed. Not only can the HSPP supply and store electrical energy according to the grid requirement but can also provide the required ancillary services, i.e. reactive power, voltage and frequency control. In addition, the power plant also possesses black start capability. The behavior of this latest HSPP structure is tested in an isolated network which contains conventional thermal and hydroelectric power plants as well as a large share of wind farms. The dynamic interaction of the HSPP with the other power plants and the roles of its internal components are analyzed in response to a step increase in power consumption in the network. The results signify that the HSPP-AC can ensure the stable operation of a grid with high penetration of renewable sources.

1   Introduction

The EU plans to be carbon neutral by the year 2050 [1]. Hence, the European Commission expects an increase in low carbon technologies in the electricity mix from about 45% at present to nearly 100% in 2050 [2]. Out of this 100% target in 2050, 50–55% would come from Renewable Energy Sources (RES) [3]. To integrate such high amounts of RES generation, significant infrastructure extensions will be necessary. Also, in order to maintain the stability of the electrical grid with only inverter-based RES, a significant portion of the inverters will need to adopt grid-forming behavior from the currently prevalent grid-following strategy. Otherwise, the intermittent RES infeed can easily destabilize an electrical network with low inertia due to higher frequency fluctuations as well as increased forecast errors [4].

Due to the stochastic nature of electrical energy generation from RES and consumption by loads, at times there is either an energy deficit or surplus in the grid. This is balanced by Conventional Power Plants (CPPs) which mostly run on fossil fuels. However, with the planned shutdown of all such fossil-fired power plants in the future, the number of synchronous machines in the electrical grid would drastically reduce, lowering the rotational inertia in the grid which is inherently responsible for grid stability [5]. To compensate for the intermittent and decentralized RES, large scale Electrical Energy Storage (EES) Systems are viable alternatives. Ideally, these

EES systems would also be expected to provide the required ancillary services, i.e. reactive power, voltage and frequency control, as well as Black Start possibilities [6]. Such a hybrid interconnected system is presented in this paper, called Hydrogen Storage Power Plant (HSPP) [7].

Currently, there are two versions of the HSPP. One consists primarily of storages and DC-DC converters (HSPP-DC). The frequency ancillary service provided by this type of the HSPP has been discussed before [8]. However, in this paper, a novel version of the HSPP consisting of storages and mainly DC-AC converters (HSPP-AC) is presented. The dynamic interaction of this new type of HSPP is tested with other RES as well as conventional thermal and hydroelectric power plants. Then the response of the HSPP-AC is compared with the HSPP-DC.

The following describes the constituent components of the two HSPP versions. This is followed by the description of the test network. The results evaluate the performance of the HSPP-AC in detail. Finally, the highlights of the investigations are then summed up in the conclusion.

2   Internal HSPP-AC Structure

The two state of the art HSPP forms are presented in **Figure 1**. In such power plants, following a sudden change in power demand or generation at the three-phase network, the tasks of providing instantaneous reserve (IR), primary and secondary control power are accomplished by its

three main storages; supercapacitor, battery and hydrogen storage respectively [9], [10], [11]. These three storages have different capacities and specific characteristics which make them ideal components to fulfill their respective tasks. The HSPP-DC, shown in **Figure 1a**, consists mainly of these three storages and DC-DC converters. The power plant is modeled in such a way that the respective DC-DC converters control the power transfer via the current flow between adjacent storages. Since the internal components in the HSPP-DC operate in DC mode, the power plant requires a DC-AC converter for grid connection.

Though the HSPP-AC uses the same three primary storages as its DC counterpart, this power plant uses DC-AC converters, which control the power transfer depending on the voltage level of these storages. It uses a supercapacitor to provide IR since the component can charge and discharge instantaneously with a high power gradient in response to network disturbances. In addition, its ability to withstand frequent charging and discharging makes it an ideal device for inertia emulation [12].

The voltage of the supercapacitor is controlled to govern the primary control power flow from the battery using the adjacent DC-AC converter. Opposed to the supercapacitor, the battery is suited for this task since it is a cheaper form of storage with a higher energy density, enabling it to supply power for a longer duration. Rapid charging or discharging of the battery is detrimental to its average lifetime and as a result, use of battery systems for providing IR is still unproven [13]. Hence, the combination of the supercapacitor in parallel to the battery ensures the required IR and primary control provisions. Additionally, a transformer is placed between the two parallel branches to protect the battery and other internal components of the HSPP-AC from electrical transients.

Both forms of the HSPP are bidirectional in nature, i.e. they can provide or store electrical energy depending on the power flow direction in the grid. The third main storage in the HSPP-AC, i.e. the hydrogen storage, is hence responsible for supplying or absorbing secondary control power. Depending on the power flow direction, either a fuel cell or an electrolyser can be used to unload or load the hydrogen storage. The power flow for each of these cases is controlled by the DC-AC converter in the respective paths between the hydrogen storage and the battery. Each of these converters are connected to series reactors to dampen the transients reaching the fuel cell and electrolyser.

While utilizing the hydrogen storage, the fuel cell generates electrical energy via the chemical reaction between stored hydrogen (H_2) and external oxygen (O_2). The reaction is exothermic and the resulting thermal energy
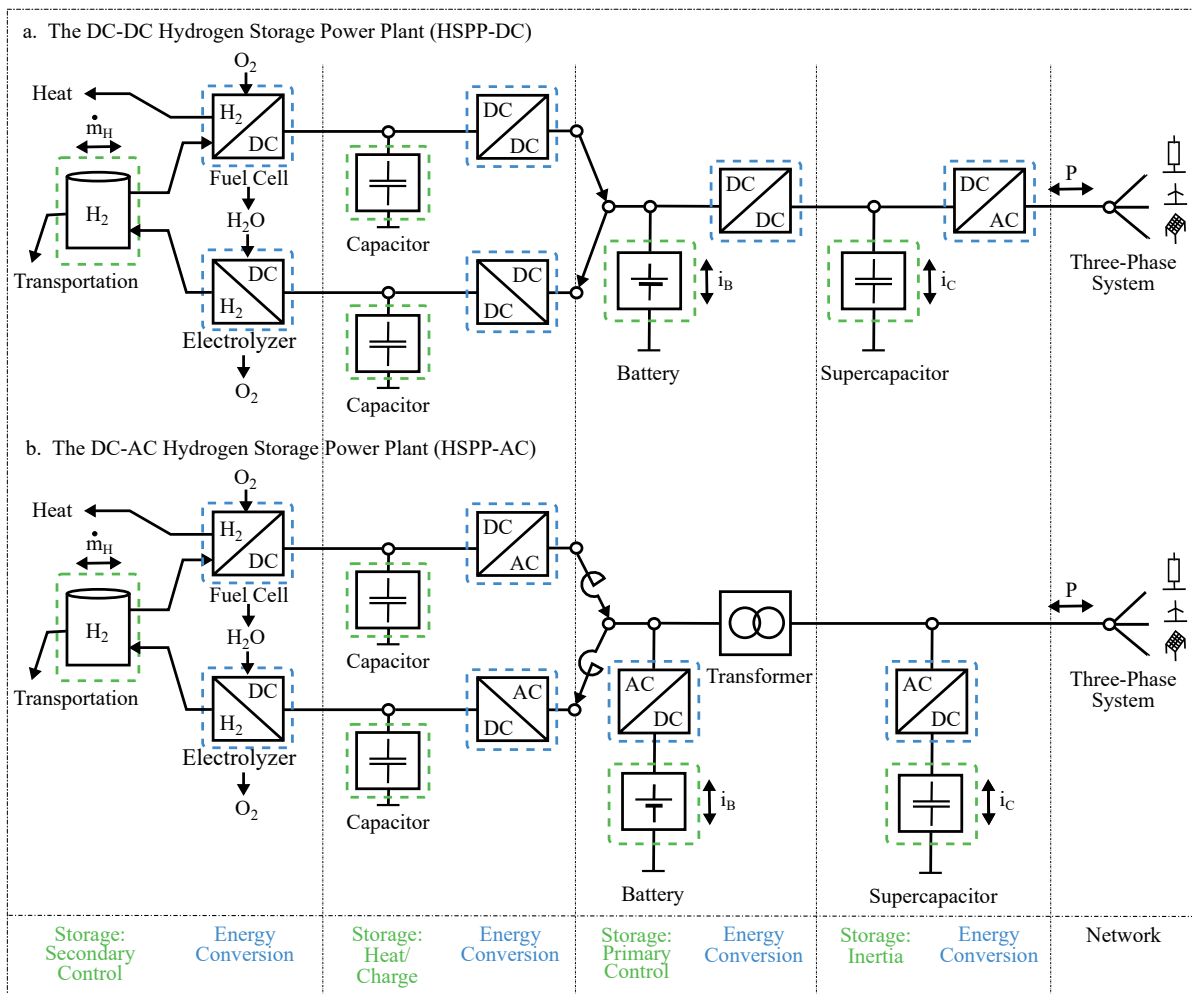

Figure 1 Comparison between the technical structures of a) HSPP-DC and b) HSPP-AC power plants

can be used for district heating. Water (H_2O), also produced due to the reaction, can serve as the electrolyte in case of a reversed power flow, i.e. surplus power feed-in from the grid. The hydrogen produced via electrolysis can be stored in a Liquid Organic Hydrogen Carrier (LOHC) system. Such a system enables safe, easy storage and transportation of hydrogen at a high energy density under ambient conditions, using the currently available infrastructure [14]. In addition to being used for electrical power generation in the HSPP, the stored hydrogen can also play a vital role in sector coupling (Power-to-X) and decarbonisation of industrial processes.

3 Test Network Description

The grid used for the investigations is shown in **Figure 2**. It consists of 25 equidistant nodes, each connected to either a power plant or a load. The nodes are interconnected via transmission lines, each 250 km long and at a voltage level of 110 kV. The line impedances are equal in magnitude with a resistance to reactance ratio of 0.1. This is a generalized grid structure that has been used for multiple research studies (including voltage-reactive power control). The purpose is to create a weak network and show that HSPPs function efficiently even under such conditions. There are eleven power plants, of which five are HSPPs (S_{AC} or S_{DC}). Amongst these five, two are HSPP-AC
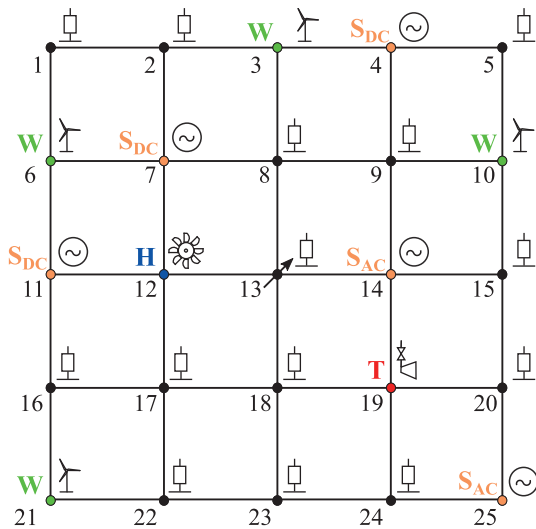
Symbol	Label	Description
🔲	-	Load
⚡	T	Thermal Power Plant
✳	H	Hydroelectric Power Plant
丅	W	Wind Power Plant
∼	S_{AC}	HSPP-AC
	S_{DC}	HSPP-DC

Figure 2 25 node electrical network

Table 1 Initial loadflow points of the network elements

Type	No.	Power setpoint (MW)	Total power (MW)
Thermal power plant	1	6	6
Hydro power plant	1	6.04	6.04
Wind power plant	4	4	16
Storage power plant	5	0	0
Total Generation	-	-	**28.04**
Loads	14	2	28
Losses	-	-	0.04
Total Consumption	-	-	**28.04**

(nodes 14 and 25) and the other three are HSPP-DC (nodes 4, 7 and 11). From the six other plants, four represent wind (W) and the other two each denote a conventional hydroelectric (H) and a coal fired thermal (T) power plant. The hydroelectric plant acts as the reference machine and meets the power losses in the system. The remaining 14 nodes each house a load, where the active and reactive power consumption are constant during the initial power flow. The loadflow setpoints for all these elements are represented in **Table 1**.

The network modeling and RMS simulations are carried out in the software DIgSILENT PowerFactory. The reactive power required by the network is supplied by the power plants but the associated results and control methods are not included in this paper due to space constraints.

4 Results and Observations

To analyze the frequency ancillary behavior of the HSPPs in combination with the other power plants, a step increase is implemented in the active power consumption for the load at node 13. The magnitude of this step is 10% of the total power consumption in the grid (28 MW) and results in a demand increase of 2.8 MW. This rise in demand is shown in **Figure 3**. Per unit values are used with an apparent power base (S_{base}) of 10 MVA.

$$\text{RoCoF} = \frac{df}{dt} = \frac{1}{T_a} \cdot (p_G - p_L) \tag{1}$$

where:

$\frac{df}{dt}$ First order time derivative of frequency (pu)

T_a Acceleration time constant (s)

p_G Total active power generated (pu)

p_L Total active power consumed (pu)

This sudden increase in total power demand leads to a negative Rate of Change of Frequency (RoCoF), as explained by (1) [15]. The corresponding frequency change in pu is displayed in **Figure 4a (top)**. The magnitude of this initial RoCoF depends on the size of the disturbance as well as the acceleration time constant

which is a representative of the power system inertia. The frequency reduction is halted by the onset of primary controller present in the CPPs and HSPPs of the grid. Next, the frequency is returned to its initial setpoint of 1 pu due to the action of the Automatic Generation Control (AGC), **Figure 4a (bottom)**. This AGC action (secondary control) is only implemented in the HSPPs in order to study their behaviour in further detail and compare the behavior of the two different versions.

Figure 4b shows the increase in active power generation of the different types of HSPPs and CPPs to meet the increased demand. The Wind Power Plants (WPPs) are represented by simple converters which keep their power output constant. The y-axis values on the left correspond to the power output values of the HSPPs, while those on the right show the same for the CPPs. This allows the IR of the power plants to be compared despite being initially at different power setpoints. The magnitude of the IR depends on the RoCoF at a particular node and the reactance of the connecting path between that node and the point of disturbance. Since the disturbance occurs at node 13, the two closest power plants, i.e. the hydroelectric plant at node 13 and HSPP-AC at node 14, provide the highest increase in power output. This exhibits that the HSPPs can contribute to inertia in the same way as the CPPs of today. **Figure 4c**, represents the power output of the power plants over a longer time scale. With the onset of secondary control, the power output of the HSPPs increase and that of the CPPs decrease, since they only possess primary control. Under steady state conditions, the increase in power demand of 0.28 pu is satisfied by the five HSPPs,

each producing 0.056 pu. The hydroelectric and thermal power plants are returned to their initial working points.

Next, the IR of the HSPP-AC at node 14 is further related to the performance of the respective storages inside the power plant. As shown in **Figure 5a** and **b**, the IR of the HSPP-AC is provided almost entirely by the supercapacitor. Consequently, the voltage of the supercapacitor decreases, **Figure 5c**, causing the battery current to increase. This increase in the battery response is referred to as the supply of primary control power by the HSPP-AC. Since the fuel cell possesses a much higher inertia compared to the battery and supercapacitor, it does not supply any additional power during this short period.

A comparison between the IR provided by the HSPP-AC and HSPP-DC can be observed in **Figure 5b** and **6a** respectively. In contrast to the HSPP-DC, the HSPP-AC has a structure more susceptible to disturbances, as shown in **Figure 1a** and **b**. Hence, some of the initial transients due to the increased demand, will reach the battery, fuel cell and electrolyser of the HSPP-AC, as presented in **Figure 6c**. However, due to the internal control implemented in this power plant and the presence of the transformer as well as the reactor coils, the magnitudes of such disturbances can be controlled to negligible values, i.e. 6% for the battery and 1.05% for the fuel cell and electrolyser respectively. Comparing **Figure 6b** and **c**, it can be inferred that the HSPP-DC does not suffer from such transients.

The active power output of the HSPP-AC at node 14 is presented over a wider time scale in **Figure 7**. Alongside, the associated roles played by its storages is also shown. During the medium time scale of 50 s, the HSPP-AC mostly supplies primary control power which originates from the battery. The product of the battery current and voltage, in **Figure 7b** and **c** denotes its output power. The battery provides sufficient electrical energy to not only meet the network demand but also recharges the supercapacitor. This recharging phase is shown by the negative supercapacitor current, visible in the upper plot of **Figure 7b**. Upon completion of this process, the supercapacitor voltage returns to its initial setpoint of 1 pu and the battery voltage continues to reduce as it provides primary control power. The charged supercapacitor can
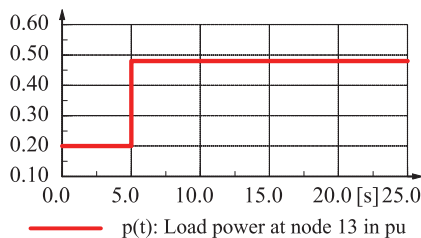
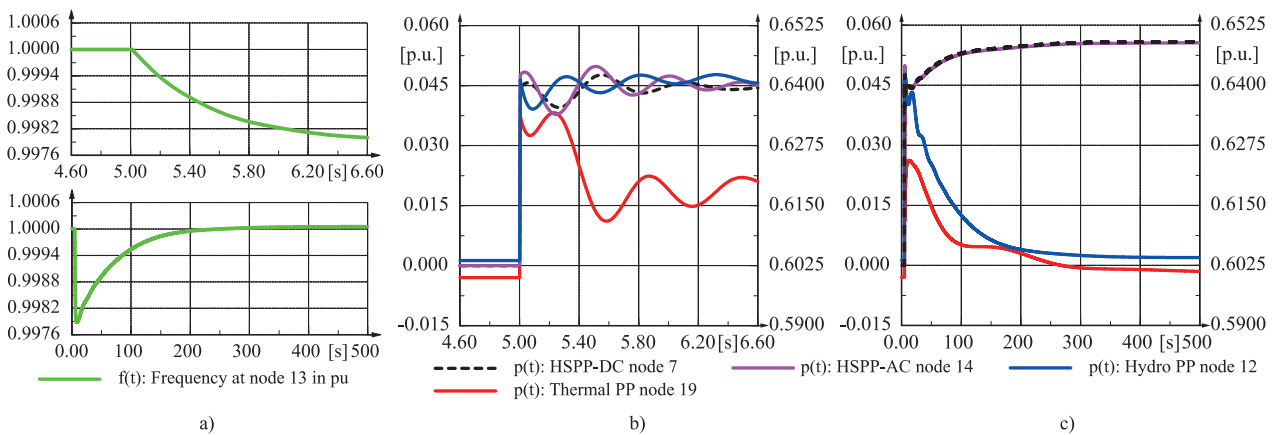**Figure 3** Step increase in power consumption at node 13

Figure 4 Frequency (a) and Active Power outputs of power plants during different time frames (b) and (c)
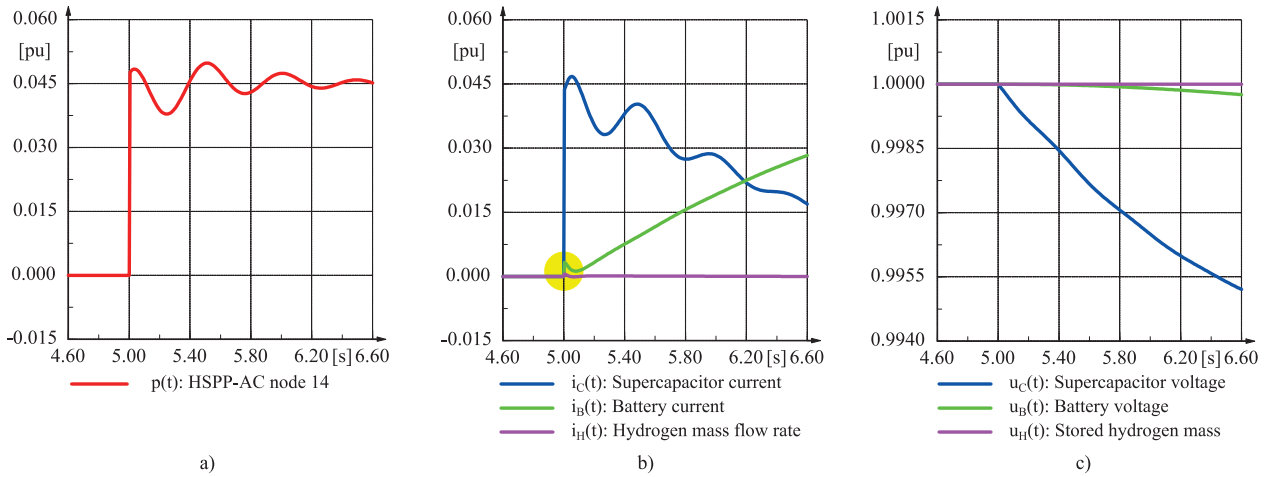
Figure 5 a) Increase in power output, b) Current flow from the HSPP-AC storages and c) Voltage levels of the storages during the initial time frame
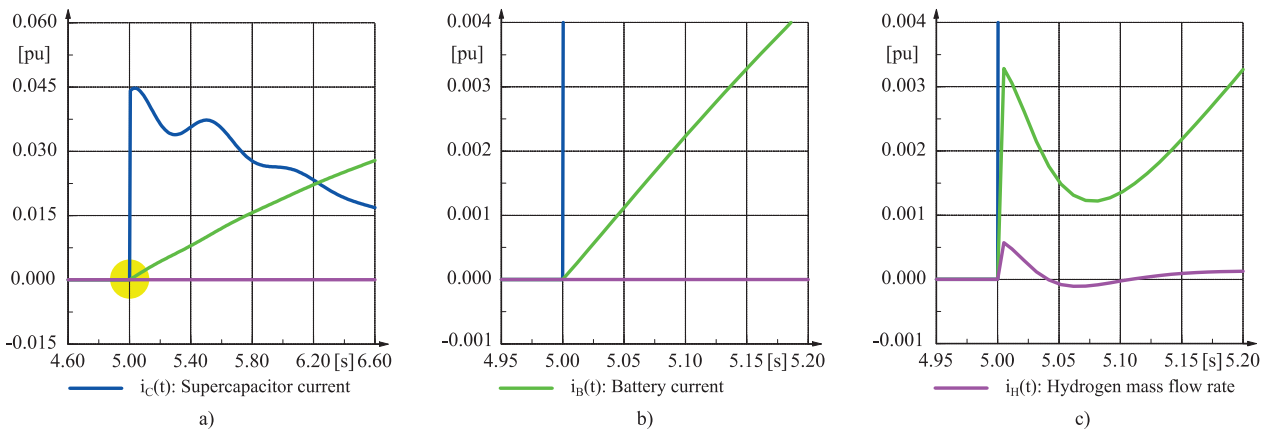

Figure 6 Current flow from the storages of a) HSPP-DC, b) Zoomed in view of a) and c) Corresponding values for HSPP-AC
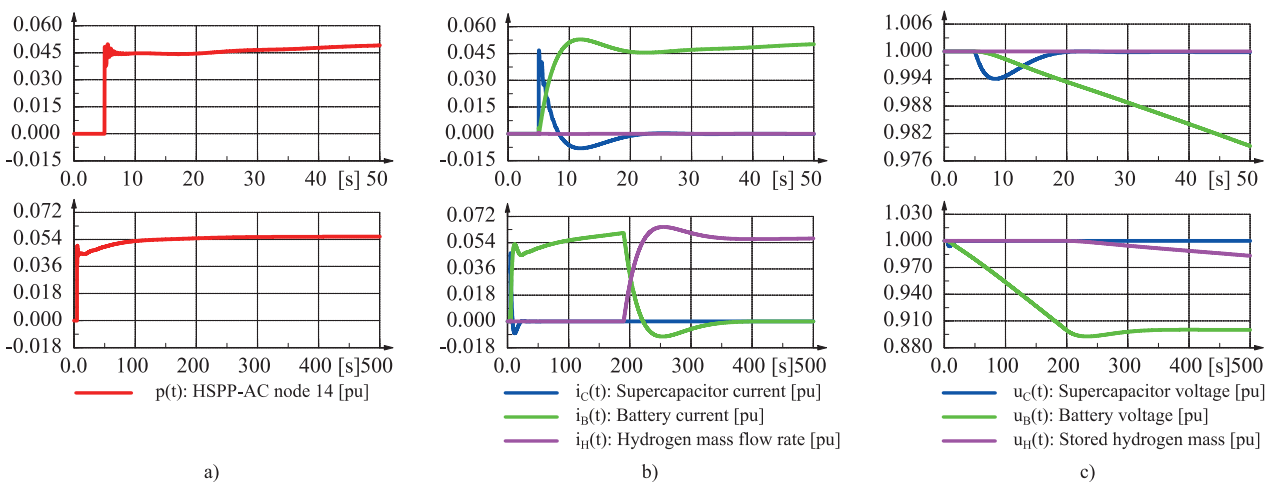

Figure 7 a) Increase in power output, b) Current flow from the HSPP-AC storages and c) Voltage levels of the storages during the medium and long time frame

once again provide the required IR incase of future disturbances in the network.

When the battery voltage, reaches the lower threshold of 0.9 pu, the DC-AC converter adjacent to the fuel cell accesses the hydrogen storage in the HSPP-AC and initiates the flow of hydrogen. This is displayed in the bottom plots of **Figure 7b** and **c**. The resulting oxidation of the hydrogen inside the fuel cell releases enough energy to balance the increased network demand and recharge the battery. This action is referred to as the supply of

secondary control power. The battery voltage is raised to permissible limits of the lower threshold and its output current is steadily brought to zero. Under steady state conditions, the fuel cell alone supplies the power demand of the three phase network using hydrogen from the storage. The supercapacitor and battery remains unused till IR or primary control power is required due to future disturbances in the grid. During surplus generation from RES, the HSPP-AC, just like its DC counterpart, can use the excess power for large-scale storage of electrical energy. The electrolyser would utilize the excess power to synthesize and store hydrogen. This could then be used as an additional reserve in sector coupling, during periods of "dark doldrums" or to overcome forecast errors.

5 Conclusion

This paper presented the dynamic interaction between the two HSPP versions, CPPs and WPPs. The novel HSPP-AC structure exhibited that it can provide the required IR, primary and secondary control, like its DC representation. Although it is slightly more prone to electrical transients compared to its DC version, it has the advantage that its components have a greater market availability. This is expected to lower its installation cost and massively aid its scale-up process. Furthermore, this novel HSPP version can also operate in distributed form with its components implemented in different areas of the electrical network. Details regarding the control scheme of the HSPP are present in [16]. The efficiency, power ratings and relative sizes of the HSPP components for a 10 MW version of the power plant are currently under discussion and will be discussed in future publications.

6 Literature

[1] EU Commission. (2020) 2050 long-term strategy. [Online]. Available: https://ec.europa.eu/clima/policies/strategies/2050_en#:~:text=The%20EU%20aims%20to%20be,action%20under%20the%20Paris%20Agreement.

[2] T. Klaus, C. Vollmer, K. Werner, H. Lehmann, and K. Müschen, "Energy target 2050: 100% renewable electricity supply," *Federal Environment Agency of Germany, Dessau-Roßlau*, 2010.

[3] I. Boie, C. Fernandes, P. Frías, and M. Klobasa, "Efficient strategies for the integration of renewable energy into future energy infrastructures in europe–an analysis based on transnational modeling and case studies for nine european regions," *Energy Policy*, vol. 67, 2014.

[4] X. Liang, "Emerging power quality challenges due to integration of renewable energy sources," *IEEE Transactions on Industry Applications*, vol. 53, no. 2, pp. 855–866, 2016.

[5] German Institute for Economic Research, *Phasing out Coal in the German Energy Sector*. DIW Berlin, 2019.

[6] J. P. Barton and D. G. Infield, "Energy storage and its use with intermittent renewable energy," *IEEE transactions on energy conversion*, vol. 19, no. 2, pp. 441–448, 2004.

[7] H. Weber, "From frequency control with inertia to angle control with converters." In German: "Von der Frequenzregelung mit Schwungmassen (netzstützende Maßnahmen) zur Winkelregelung mit Umrichtern (netzbildende Maßnahmen)," 2017.

[8] H. Weber, "The ancillary response of storage power plants in the present and future electrical grid," in *Energy Transition in Power Supply - System Stability and System Security; 13th ETG/GMA-Symposium*, 2019.

[9] H. Weber, N. Ahmed, M. Töpfer, P. Gerdun, and V. Vernekar, "Dynamic behavior of conventional and storage power plants in a single power system," in *2019 IEEE Milan PowerTech*. IEEE, 2019, pp. 1–6.

[10] P. Gerdun, N. Ahmed, V. Vernekar, M. Töpfer, and H. Weber, "Dynamic operation of a storage power plant (spp) with voltage angle control as ancillary service," in *2019 International Conference on Smart Energy Systems and Technologies (SEST)*. IEEE, 2019, pp. 1–6.

[11] M. Töpfer, N. Ahmed, and H. Weber, "Dimensioning the internal components of a hydrogen storage power plant," in *2020 International Conference on Smart Energy Systems and Technologies (SEST)*. IEEE, 2020, pp. 1–6.

[12] R. Zhang, J. Fang, and Y. Tang, "Inertia emulation through supercapacitor energy storage systems," in *2019 10th International Conference on Power Electronics and ECCE Asia (ICPE 2019-ECCE Asia)*. IEEE, 2019, pp. 1365–1370.

[13] M. G. Dozein and P. Mancarella, "Frequency response capabilities of utility-scale battery energy storage systems, with application to the august 2018 separation event in australia," in *2019 9th International Conference on Power and Energy Systems (ICPES)*. IEEE, 2019, pp. 1–6.

[14] D. Teichmann, W. Arlt, P. Wasserscheid, and R. Freymann, "A future energy supply based on liquid organic hydrogen carriers (LOHC)," *Energy & Environmental Science*, vol. 4, no. 8, pp. 2767–2773, 2011.

[15] P. S. Kundur, N. J. Balu, and M. G. Lauby, "Power system dynamics and stability," *Power System Stability and Control*, vol. 3, 2017.

[16] Prof. Dr.-Ing. Harald Weber, "External and internal control of a storage power plant operating without rotating masses." In German: "Verfahren zur exteren und internen Regelung eines schwungmasselosen Speicherkraftwerks," Patent number: **10 2019 124 268.1**.